Heterogeneities of the Earth's inner core boundary by pre-critically reflected phases of PKiKP and PcP

Dmitry Krasnoshchekov[1], Vladimir Ovtchinnikov[1] and Valentin Polishchuk[2]

[1]Institute of Dynamics of Geospheres, Russian Academy of Sciences, Moscow, Russia, krasnd@idg.chph.ras.ru

[2]Department of Science and Technology, Linköping University, SE 60174 Norrköping, Sweden

AGU 100 FALL MEETING Washington, D.C. | 10–14 Dec 2018

DI43B-0017

I. Introduction

PKiKP is the wave reflected off the inner core boundary (ICB) and PcP - off the core-mantle boundary (CMB). Differential measurements of PKiKP and PcP give insight into the structure and properties of the Earth's core. The PKiKP/PcP amplitude ratio yields the ICB density jump estimate [Bolt&Qamar, 1970] and PKiKP-PcP differential travel times are sensitive to the outer core thickness. The PKiKP-PcP differential measurements have provided lots of estimates of physical parameters of substances compounding the ICB and CMB as well as their topography. However, lack of amplitude ratios measured after the steepest reflections (or at short epicentral distances) is still a challenge mostly because amplitudes of such narrow angle reflections are tiny.

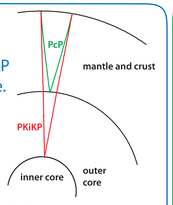

Fig. 1. Ray path geometry for seismic phases PKiKP and PcP

II. Data & Differential travel time measurements

We revisit heterogeneities of ICB using the database of a total of more than 1300 new differential travel times and amplitude ratios of PKiKP and PcP measured at 3.2°–35.2° and reflected off two spots in the western and eastern hemispheres of the Earth's core. Pre-critical PKiKP and PcP waveforms were successfully detected on broadband and short-period records of four deep earthquakes. The reflection points of the analysed dataset provide good sampling of two IC spots of about 125 x 240 km^2 under Bolivia and to the southeast of Sakhalin Island (Fig. 2). Each spot is probed by hundreds of ray traces with incident angles from 2° to 20°. To uniform the analysed dataset and increase signal-to-noise ratio of PKiKP and PcP waveforms, raw digital traces were frequency-filtered between 1.1 and 7 Hz. The filtering removed intensive crust and mantle reverberations and accentuated the detected pulse-shaped waveforms of PcP and PKiKP on vertical components. The revealed PKiKP and PcP waveforms build hyperbolic travel time curves, characteristic for the reflected phases (Fig. 3). After filtering, both PKiKP and PcP waveforms dominate on the time interval tens of seconds long around the predicted arrival time and exhibit signal-to-noise ratios well above 2.5.

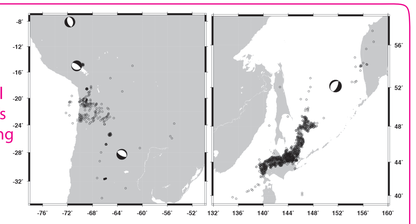

Fig. 2. Map with epicentres of analysed earthquakes (beach balls) and daylight surface projections of PKiKP reflection points (circles). Right panel shows 1074 points sampling the IC surface in its eastern hemisphere, left – 256 bounce points in the western.

Fig. 3. Record section plot of 18 frequency-filtered vertical components (station names are on the right). Left pane: passage corresponding to arrival of PcP; right pane: to PKiKP. Standard travel time curves of PcP and PKiKP are computed for ak135.

We find that PKiKP–PcP differential travel time residual with respect to a standard Earth model measured in the eastern hemisphere are by 0.72 s below the ones in the West, which can mean (Shen et al., 2016) the OC under the Americas is about 3 km thicker than under Southeastern Asia. Concretely, the mean PKiKP–PcP differential travel time residuals calculated with respect to ak135 and PREM over 1016 Japanese records were, respectively, –1.79 s and –0.41 s with s.d. of 0.51; same estimates for the western hemisphere made –1.07 ± 0.45 s and 0.31 ± 0.45 s. This estimate of OC thickness variability is rather an upper bound subject to allowance for ellipticity and possible influence of strongly heterogeneous lower mantle. Here we address 3-D high-resolution tomographic model of LLNL-Earth3D that takes into account Earth's ellipticity, undulating discontinuity surfaces and heterogeneities in mantle and crust. The qualitative analysis predicts that crust and mantle heterogeneities have essentially similar influence on almost vertically propagated PKiKP and PcP (e.g. at 3.2°, where the respective Fresnel zones are larger than separation between the PcP and PKiKP pierce/reflection points), but act differently a little farther, where PKiKP and PcP paths start to diverge in lower mantle. It is this pattern that we observe in Fig. 4. Above the epicentral distance of 16.5°, the measured residuals didactically follow the behaviour predicted by LLNL-Earth3D and therefore mostly contain information on heterogeneities outside the Earth's core. To decrease data contamination with non-core effects, we examined the statistics on residuals obtained only under 16.5° and the mean of residuals calculated over 330 reflections in the East and 181 in the West were –0.45 ± 0.55 s and 0.27 ± 0.44 s, accordingly, while the modelled residuals made –0.27 ± 0.07 s and 0.12 ± 0.10 s. These averages indicate that up to a half of the systematic bias between PKiKP–PcP differential travel time residuals measured in eastern and western hemispheres can be accounted for by out-of-core structures, still the rest of the bias is induced by the Earth's core, statistically significant and equivalent to hemispherical disparity in OC thickness of about 1–3 km.

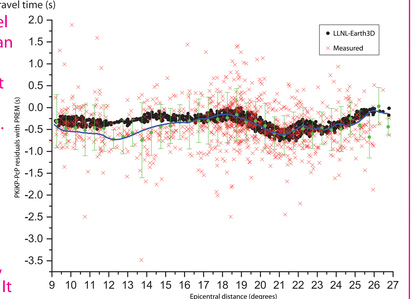

Fig. 4. Differential travel time residuals for 1016 records collected in Japan. Green dots with standard deviation bars are 0.5° binned averages of measured residuals. Blue line – alpha-shape reconstructed distance dependence of measured residuals.

III. PKiKP/PcP amplitude ratio

A method for estimating inner core boundary density jump by using PKiKP/PcP amplitude ratio was proposed more than 40 years ago [Bolt & Qamar, 1970]. They used a system of three equations with three unknowns for the inner core boundary (Fig. 5 and Fig. 6). $\alpha 1$ and $\rho 1$ are the compressional velocity and density of the liquid, while $\alpha 2$, $\beta 2$ and $\rho 2$ are the compressional and shear velocities and density of the solid core. A similar system can be written for the core-mantle boundary. The systems explicitly include density ratio $\rho 1/\rho 2$. The angles of incidence, reflection and transmission coefficients depend on the elastic parameters and the epicentral distance. At short epicentral distances PcP and PKiKP ray paths are nearly identical in mantle and an expression for PKiKP/PcP displacement ratio as a function of epicentral distance can be written as in Fig. 7, where $\eta_S(\Delta)$ and $\eta_Q(\Delta)$ are geometrical spreading and attenuation correction factors, accordingly. Estimates of the density jump by various authors resulted in a diversity values in the range of 0.45 ÷ 1.8 g/cm^3 [Souriau & Souriau, 1989; Ovtchinnikov et al., 1997; Koper & Pyle, 2004; etc.].

$$\begin{vmatrix} \beta_2(\tan^2\varphi_3 - 1) & 0 & 2\alpha_2 \tan\varphi_2 \\ \beta_2 & -\alpha_1 \tan\varphi & -\alpha_2 \tan\varphi_2 \\ 2\frac{\beta_2^3}{\alpha_1^2}\tan\varphi_3 & \frac{\rho_1}{\rho_2}\alpha_1 \sec^2\varphi & -\alpha_2\frac{\beta_2^2}{\alpha_1^2}(\tan^2\varphi_3 - 1) \end{vmatrix} \begin{vmatrix} B/A \\ C/A \\ D/A \end{vmatrix} = \begin{vmatrix} 0 \\ -\alpha_1 \tan\varphi \\ -\frac{\rho_1}{\rho_2}\alpha_1 \sec^2\varphi \end{vmatrix}$$

Fig. 5. A system for liquid-solid interface and waves shown in Figure 6, that is build on the base of boundary conditions: (i) normal displacements are continuous, (ii) tangential stresses vanish and (iii) normal stresses are continuous.

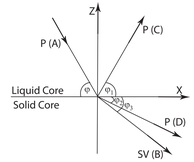

Fig. 6. Reflection and transmission of seismic waves on the inner-outer core boundary.

$$\frac{\mathcal{A}(PKiKP)}{\mathcal{A}(PcP)}(\Delta) = \frac{\mathcal{T}_{CMB\text{-}D}(\Delta)\,\mathcal{R}_{ICB}(\Delta)\,\mathcal{T}_{CMB\text{-}U}(\Delta)}{\mathcal{R}_{CMB}(\Delta)}\,\frac{\eta_Q(\Delta)}{\eta_S(\Delta)}$$

$$\eta_S(\Delta) = \sqrt{\frac{\cos^2 i_{PKiKP}}{\cos^2 i_{PcP}}\,\frac{p_{PcP}}{p_{PKiKP}}\left|\left(\frac{dp}{d\Delta}\right)_{PcP}\Big/\left(\frac{dp}{d\Delta}\right)_{PKiKP}\right|}$$

$$\eta_Q(\Delta) = \exp(-\pi\Delta t/QT)$$

Fig. 7. Dependence of PKiKP/PcP amplitude ratio on epicentral distance. T and R are upward (-U) and downward (-D) transmission and reflection coefficients of primary waves on inner-outer core (ICB) and core-mantle (CMB) boundaries.

IV. Results & Discussion

Theoretical curves of various ICB density jump models are not far apart (especially above 10°), whereas the scatter of measurements is large (Fig. 8). In addition, as argued above, it's reasonable to include only data under 16.5° (since above this limit the ratios may suffer from influence of heterogeneities outside the Earth's core). Figure 9 shows that eastern and western measurements up to epicentral distances of about 16° are consistently divided by a gap equivalent to the ICB density jump of about 0.6 g/cm^{-3}. Given the notorious trade-off between variation of acoustic impedance contrast at ICB and CMB, and the resulting ICB density jump estimate, an alternative interpretation in terms of CMB density jump has to be examined too. The interpretation would assume 10 to 15 percent density variation between the probed western and eastern spots of the mantle bottom (Fig. 9). However, such variation can be controversial in geodynamical context because the sampled mantle sides of CMB feature essentially similar shear velocities (Fig. 10) and material properties specific to regions outside the Pacific large low-shear-velocity province. Strong density variations on the core side of CMB are hardly possible too. Essentially similar considerations are valid for interpretations of CMB/ICB trade-off in terms of velocity. If we appeal to CMB variation only, we should suggest strong lateral changes in velocity contrast between about 4.8 and 5.5 km/s under Southeastern Asia and almost constant velocity jump of about 5.75 km/s in South America (Fig. 11). However, such pattern is not supported by global P-wave models including LLNL-Earth3D that, as shown above, secures good prediction of measured PKiKP-PcP differential travel times. For both spots (Fig. 12) they suggest almost equal P-wave velocities few tenths of percent below the ones in standard models that envisage the negative velocity jump from mantle to core of about 5.65 km/s in absolute value.

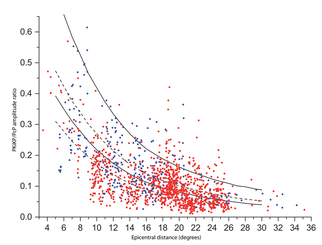

Fig. 8. Measured PKiKP/PcP amplitude ratios and their theoretical estimates for ak135. Red and blue dots – measured ratios in eastern and western hemispheres, respectively. Theoretical curves are for ICB density jumps of 0.3 g/cm^3 (lower dash), 0.6 g/cm^3 (lower solid), 0.9 g/cm^3 (upper dash), 1.8 g/cm^3 (upper solid).

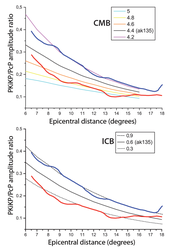

Fig. 9. Theoretical and observed dependencies of PKiKP/PcP amplitude ratio on distance. Theoretical curves on the base of ak135 are for varying ICB and CMB density jumps given in the legends in g/cm3. Thick red and blue lines are the k-order α-shape distance dependencies reconstructed from the eastern and western subsets, respectively.

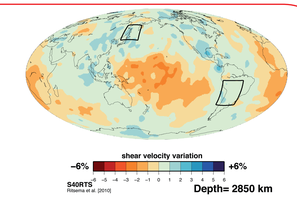

Fig. 10. Shear velocity distribution on the mantle side of CMB in conformity with S40RTS20. Black boxes delineate the areas sampled by reflected waves from our dataset.

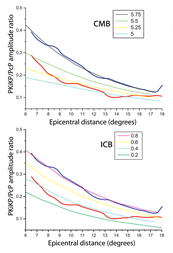

Fig. 11. Theoretical and observed dependencies of PKiKP/PcP amplitude ratio on distance. Theoretical curves on the base of PREM are for varying ICB and CMB velocity jumps given in the legends in km/s. Thick red and blue lines are the α-shape distance dependencies reconstructed from the eastern and western subsets, respectively.

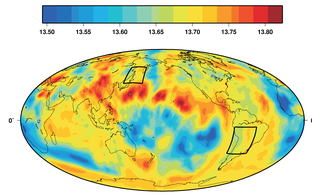

Fig. 12. P-wave velocity distribution on the mantle side of CMB in conformity with LLNL-Earth3D. Black boxes delineate the areas sampled by reflected waves from our dataset. The velocity unit of the colour scale bar is in km/s.

V. Conclusions

The analysed reflected data indicate dissimilarity of two spots of the Earth's core sampled in its eastern and western hemispheres. Beyond concoctions connecting the observations to multifactorial contributions of out-of-core inhomogeneities, we are motivated to consider a model with variable ICB density jump. We estimate it to be about 0.3 g/cm^3 under Southeastern Asia, and about 0.9 g/cm^3 under South America. Finding out whether it is a sign of IC dichotomy or mosaic character of the IC surface is not possible by means of the presented dataset. Neither mosaic nor dichotomy is preferred, but a simple degree-one global ICB density jump distribution would go in line with previously established hemispherical differences in the bulk IC. Together with variable OC thickness inferred from differential travel times, the distribution would comply with crystallisation in the denser cold western hemisphere and melting on the opposite hot eastern side (Alboussièr et al., 2010; Monnereau et al., 2010), and not vice versa as argued by Aubert et al. (2008).

VI. References

Aboussiére et al., *Nature*, **466**, 744–747, 2010.
Aubert et al., *Nature*, **454**, 758-761, 2008.
Bolt & Qamar, *Nature*, **228**, 148-150, 1970
Buchbinder & Poupinet, *BSSA*, **63**, 2047-2070, 1973.
Koper & Pyle, *JGR*, **109**, B03301, doi:10.1029/2003JB002750, 2004.
Monnereau et al., *Science*, **328**, 1014–1017, 2010.
Ovtchinnikov et al., *Doklady Earth Sciences*, **354**, 595-599, 1997.
Shen et al. *Phys. Earth Planet.Inter*, **252**, 37-48, 2016.
Souriau & Souriau, *GJI*, **98**, 39-54, 1989.
Tkalcic et al., *GJI*, **179**, 425-443, 2009.

VII. Acknowledgement

THIS WORK IS SUPPORTED BY THE RUSSIAN FOUNDATION FOR BASIC RESEARCH GRANT #18-05-00619.